Proceedings of GT2006
ASME Turbo Expo 2006: Power for Land, Sea and Air
May 8-11, 2006, Barcelona, Spain

GT2006-90434

THE EFFECT OF STAGGER VARIABILITY IN GAS TURBINE FAN ASSEMBLIES

Mark J. Wilson and Mehmet Imregun
Centre of Vibration Engineering
Department of Mechanical Engineering
Imperial College London
SW7 2BX
United Kingdom

Abdulnaser I. Sayma
School of Engineering and Design
Howell Building
Brunel University, Uxbridge
Middlesex UB8 3PH
United Kingdom

ABSTRACT

Fan blades of high bypass ratio gas turbine engines are subject to substantial aerodynamic and centrifugal loads, producing the well-known phenomenon of fan blade untwist. The accurate prediction of the running geometry, as opposed to the cold geometry at rest, is crucial in the assessment of aerodynamic performance, vibratory response and noise production of the fan. The situation is further complicated by the fact that some geometric variation is inevitable even for the state-of-the-art manufacturing processes used. The aim of this paper is to investigate the effect of static stagger variability on the dynamic untwist behaviour of fan assemblies. An aeroelastic model was used to show that under certain conditions the stagger pattern changes significantly, both in form and amplitude, relative to the static configuration. At other conditions, a strong correlation between the running and static patterns is demonstrated. [*Keywords*: stagger variability, stagger pattern, untwist]

NOMENCLATURE

CF	Centrifugal
U	Total untwist
U_{CF}	Untwist due to centrifugal loads
U_p	Untwist due to aerodynamic loads
ϕ_r	Running tip stagger
ϕ_s	Static tip stagger

1 INTRODUCTION

As an assembly of high aspect ratio, thin, flexible aerofoils rotates, the centrifugal and aerodynamic loads deform the blades relative to their stationary shape. Such assemblies are typically found in the fan system of gas turbine engines powering large civil airframes. The deformation induced by the running forces can reduce the tip stagger of the blades by around 5 degrees, producing the well known phenomenon of fan blade untwist. Untwist is defined as the difference between the static and running tip stagger of the fan,

$$U = U_{CF} + U_p = \phi_s - \phi_r,$$

where the symbols are defined in the nomenclature. Typically, fan blades open up under the aerodynamic and centrifugal loads, resulting in a positive value of untwist. At sea-level, where the aerodynamic loads are high, the deformation induced is greatest.

The accurate prediction of the running geometry of a fan is a crucial step in the design process. Incorrectly predicting the untwist of a fan will result in the blades assuming the wrong aerodynamic shape under running conditions. Geometric variation due to manufacturing and assembly processes are ignored during design and it is inherently assumed that all blades in the assembly are identical.

Blade-to-blade geometric variability has been theoretically shown to alter the vibratory response to aerodynamic excitation [1], enhance flutter stability [2] and generate multiple pure tone or buzz saw noise [3]. Experimentally, the performance of

a fan assembly has been shown to be influenced by blade-to-blade geometric variations [4]. It has also been noted during shock visualisation experiments that the position of the shock waves forming on the suction side of transonic aerofoils may be sensitive to geometric variations [5]. However, to the best of the authors' knowledge, all analyses of geometric variability ignore the additional change in blade shape induced by the varying aerodynamic loads arising from geometric blade-to-blade variability. The aim of this paper is to investigate the effect of static stagger variability on the dynamic untwist behaviour of fan assemblies.

The remainder of this paper is structured as follows. First, a discussion of the aeroelastic model used in the computational study is given, followed by a description of the transonic fan analysed. The untwist results of a nominal assembly are then presented, followed by a discussion of the behaviour of a mis-staggered fan assembly.

2 AEROELASTIC FORMULATION

To determine the running geometry of a fan blade, the deflections arising form the aerodynamic and structural loads must be calculated. There are three major computational methods that can be applied to this problem: fully coupled, closely coupled and loosely coupled analyses [6]. Fully coupled analyses involve integrating the structural and aerodynamic equations simultaneously, and are computationally very expensive. The loosely coupled analysis technique involves iteratively applying aerodynamic and structural solvers, a method adopted by Yamamoto and August [7] and Srivastava et al. [8]. This method involves passing surface pressures derived from the aerodynamic solution to the structural solver. Blade displacements can then be calculated, and a new blade shape generated for aerodynamic analysis. This process is repeated until the change in blade displacements from one iteration to the next falls below a predetermined convergence level.

Alternatively, the structure and the fluid can be closely coupled through the use of an integrated aeroelastic code. The closely coupled method is an efficient technique for solving complex nonlinear problems, and is the most widely used method in the field of aeroelasticity. Guruswamy [9] and Marshall [10] have successfully applied the integrated technique, and it is the method adopted here. The computational study presented in this paper was performed using an integrated non-linear aeroelastic code that couples a non-linear CFD model to a linear modal model of the structure. The details of the code along with case studies are reported by Sayma et al. [11, 12].

The first step in the application of the aeroelastic code to the problem of untwist prediction is as follows. A finite element structural code is used to calculate the blade deformations induced when the assembly is rotating in a vacuum. A modal analysis is also performed and the dominant low frequency vibration modes extracted, forming the basis of the linear modal model of the structure implemented in the aeroelastic code.

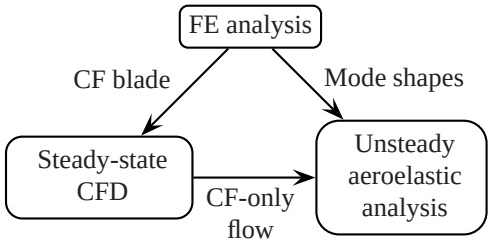

Figure 1. UNTWIST PREDICTION METHOD

Next, the steady-state flow solution around the centrifugally displaced blades is calculated. At this stage the blades are held fixed and are not allowed to deform in response to the aerodynamic loads. Such a configuration can be viewed as modelling very low density flow around the assembly, in which the interaction between the aerodynamics and the structure is very weak. Once the steady-state solution is obtained, corresponding to the geometry deformed by centrifugal loads but not aerodynamic loads, the system can be marched forward in a time-accurate fashion to find the effect of the real aerodynamic loads. In this, the pressure loads and blade displacements are exchanged between the aerodynamic and structural models at every time-step. When the system reaches equilibrium, that is the steady deformation with no further vibrational motion, the untwist of the blade is determined. The structure is usually damped just below critical levels so that the untwist position can be obtained with minimum oscillation about the final position of equilibrium. Figure 1 summarises the adopted untwist prediction method.

The aerodynamic mesh used for this computational study is semi-structured in form, being structured in the radial direction and unstructured in the axial and tangential directions [13]. The blade surface is treated as a viscous boundary and is surrounded by a structured hexahedral O-mesh to resolve the large gradients normal to the wall effectively. The near-wall flow is approximated through the application of wall functions with a slip velocity at the wall. The one equation turbulence model of Spalart and Allmaras [14] is used to calculate the eddy viscosity. For the cases including the gap between the tip of the blade and the casing, the hub and casing are treated as viscous walls. When the tip gap is omitted from the model, the end-walls are treated as inviscid boundaries.

During the unsteady aeroelastic calculation, the blade deforms under the aerodynamic loads. To accommodate this motion, the CFD mesh needs to be deformed at each time-step. To achieve this, each edge of the mesh is assigned a stiffness and treated as a spring, a method first developed by Batina [15] and Robinson et al. [16]. As the blade moves, a Jacobi iteration scheme is used to calculate the displacement at each node from force balance considerations. To maintain the integrity of the mesh as the blade moves, the stiffness of an edge is set to be

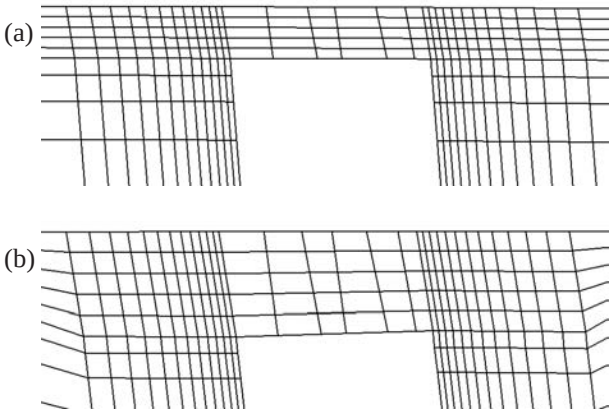

Figure 2. PROJECTION OF TIP GAP MESH ONTO PLANE NORMAL TO TIP STAGGER LINE AT 7% CHORD, (a) BEFORE AND (b) AFTER A TYPICAL DEFORMATION.

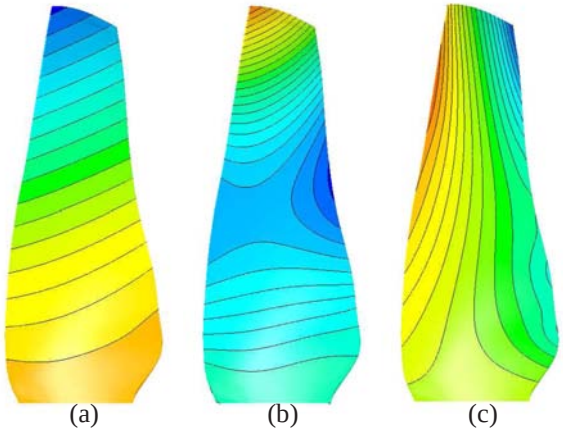

Figure 3. DOMINANT LOW FREQUENCY MODE SHAPES. (a) FIRST FLAP, (b) SECOND FLAP, (c) FIRST TORSION

Aspect ratio (height / mid-height chord)	2.3
Bypass ratio	5 to 7
Number of blades	26
Tip stagger	63° to 68°

Table 1. TRANSONIC FAN PARAMETERS

inversely proportional to the square of its length. This ensures that the bulk of the blade motion is absorbed in the larger cells that can tolerate the largest deformation without collapse. To maintain mesh integrity during large scale deflections, the points on the casing must be allowed to slide along the casing surface.

As well as large displacements in the circumferential direction as the blade deforms in response to the aerodynamic loads, the tip will move radially relative to the casing. For the inviscid end-wall model, the motion of the blade normal to the casing is ignored, ensuring that the blade tip remains on the casing line. For the cases including the tip-gap, the extent of the tip-gap will vary as the blade untwists. As a result, the mesh above the blade is redistributed to maintain an even distribution of points radially. Figure 2 shows the projection of the mesh onto a plane normal to the tip stagger line before and after a typical deformation.

3 CASE STUDY DESCRIPTION

The coupled aeroelastic code presented above was applied to a typical transonic fan designed to power a large civil airframe. The details of the blading are listed in table 1. The dominant low frequency mode shapes spanning frequencies from 50Hz to 200Hz used in the analysis are shown in Fig. 3.

A characteristic feature of the flow around a transonic fan is the presence of a shock wave near the tip of the blade. The position of the shock wave changes as the rotational speed of the fan is varied, producing complex shock structures. The position of the shock strongly influences the lift distribution over the aerofoil surface, and hence impacts the untwist generated by the aerodynamic loads, the “pressure untwist”. At low shaft speeds the shock forms on the suction surface of the blade ahead of the passage; the shock is “expelled” from the blade passage and the flow is “unstarted”. At high rotational speeds the shock moves rearward and forms in the blade passage itself; the shock is “swallowed” and the flow is “started”. To investigate the dynamic untwist behaviour of the fan, three operating points will be used; unstarted, started, and an intermediate condition between the two flow regimes. Static pressure contours at the three flow regimes on the casing of the fan are shown in Fig. 4.

Aside from the position of the shock relative to the blade, the altitude at which the fan operates greatly influences the aerodynamic loads and hence the pressure untwist. The low pressure, low density air at a typical cruise altitude near the edge of the troposphere induces only a small pressure untwist. Operating the fan at sea-level greatly increases the aerodynamic forces on the aerofoil, generating higher levels of pressure untwist. Hence the blade-to-blade variation in aerodynamic loads arising from geometric variability will be greatest at this operating condition. As a result, all calculations are performed under sea-level conditions.

To ascertain the density of the aerodynamic mesh required to produce acceptably accurate untwist results, a mesh sensitivity study was carried out using two mesh densities. It was found that increasing mesh size by a factor of two only marginally influenced the predicted untwist and aerodynamic performance, as shown in Fig. 5 and Fig. 6. The isentropic efficiency of

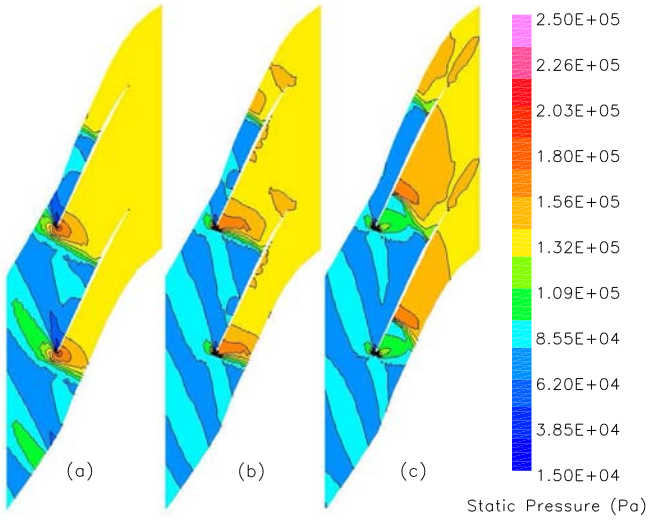

Figure 4. CASING STATIC PRESSURE CONTOURS, NOMINAL BLADE, NO TIP-GAP. (a) UNSTARTED, (b) INTERMEDIATE, (c) STARTED FLOW.

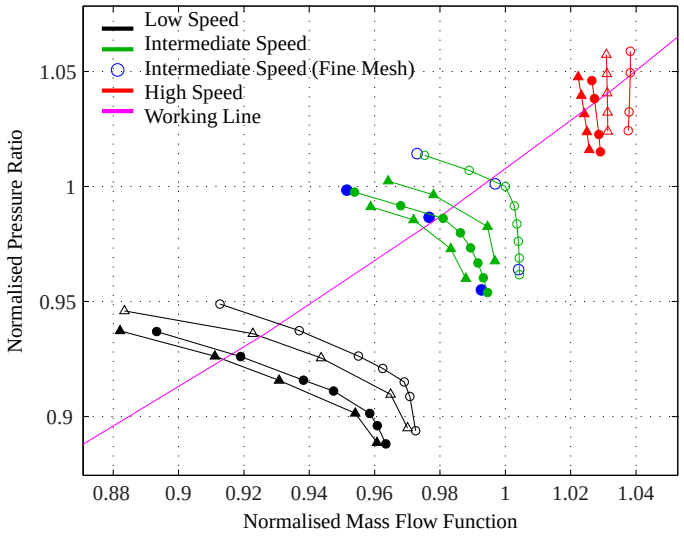

Figure 5. FAN CHARACTERISTICS (▲: CF-ONLY WITH TIP GAP, △: CF+GAS WITH TIP GAP, ●: CF-ONLY WITHOUT TIP GAP, ○: CF+GAS WITHOUT TIP GAP)

the fan was also relatively insensitive to the mesh used, the largest discrepancy of 0.36% occuring at peak efficiency, the mean descreapancy being 0.19%. As a result of this study, the coarser mesh containing approximately 200,000 and 320,000 points per blade passage for the inviscid and viscous end-wall models respectively was adopted for the analysis.

4 NOMINAL ASSEMBLY RESULTS

Before a discussion of the effects of stagger variability is given, it is useful to investigate the untwist behaviour of a nominal assembly at the desired operating points. To analyse a mis-staggered assembly, all blades in the assembly must be included in the model. However, if all blades are identical, only a single passage is required with appropriately defined periodic boundaries. As such the model size and hence computational effort required is greatly reduced, allowing a wider range of conditions to be analysed. Exploiting this, the analyses at the three speeds giving rise to unstarted, started and the intermediate flow regimes was extended to generate constant speed characteristics. In reality, a characteristic is generated by changing the size of the exit nozzle of the fan. Computationally this is achieved by modifying the static pressure profile prescribed at the exit boundary. The shaft speeds producing unstarted and started flow on the working line are denoted “low” and “high” respectively.

The fan characteristics are shown in Fig. 5 for blades displaced by the centrifugal forces only (denoted as “CF only”), and for blades displaced by both centrifugal and aerodynamic

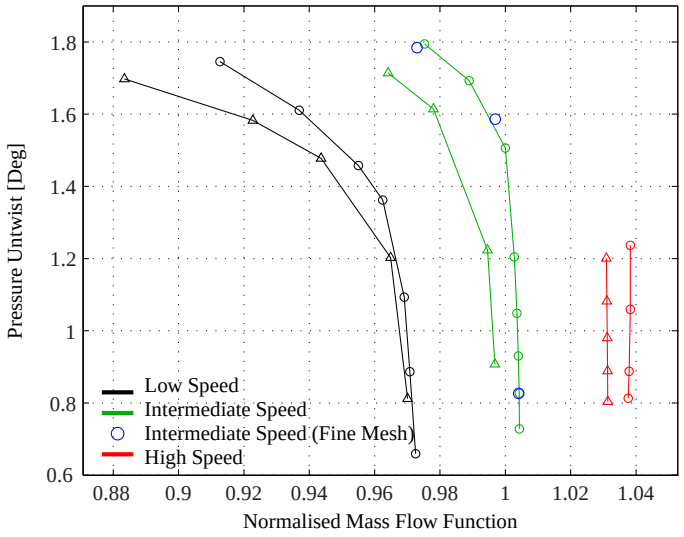

Figure 6. FAN UNTWIST (△: CF+GAS WITH TIP GAP, ○: CF+GAS WITHOUT TIP GAP)

loads (denoted as “CF + gas”). Results for models including and excluding the tip-gap are shown. The corresponding pressure untwist for each case is shown in Fig. 6, and the CF-only and CF+gas tip static pressure distributions for the working line points are shown in Fig. 7 and Fig. 8 respectively.

One main difference between the CF-only and the CF+gas characteristics is in the mass-flow rate passing through the fan.

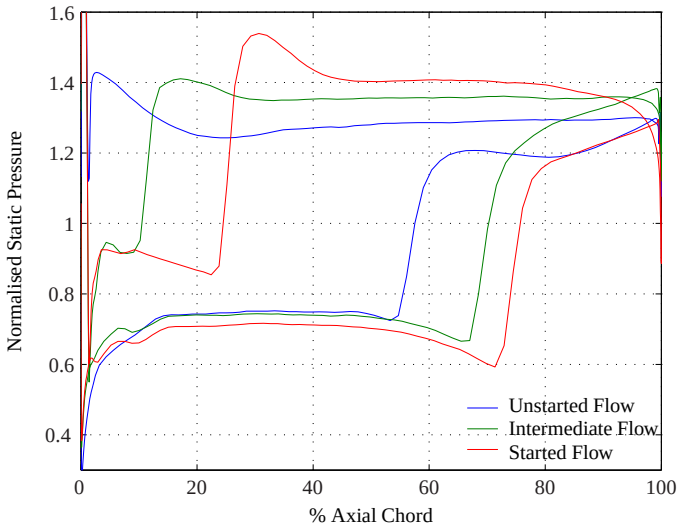

Figure 7. FAN BLADE STATIC PRESSURE DISTRIBUTIONS ON WORKING LINE, CF-ONLY WITHOUT TIP-GAP, 91% HEIGHT.

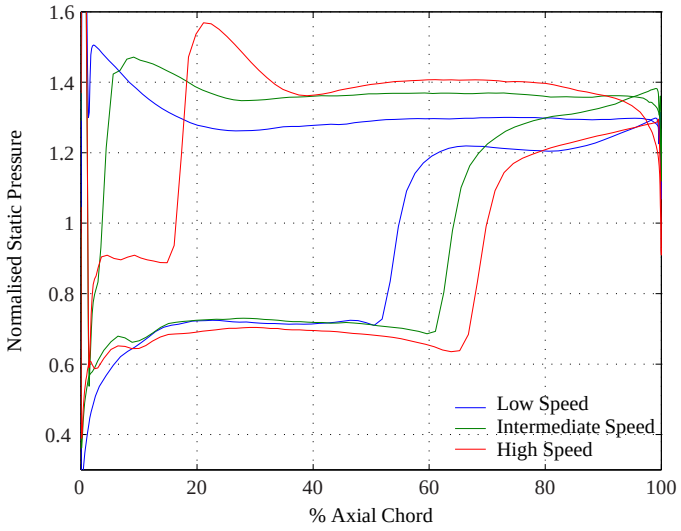

Figure 8. FAN BLADE STATIC PRESSURE DISTRIBUTIONS ON WORKING LINE, CF+GAS WITHOUT TIP-GAP, 91% HEIGHT.

As the fan untwists in response to the aerodynamic loads, the stagger reduces and the blades turn toward the axial direction. This increases the throat area of the fan, and hence the mass-flow rate increases, shifting the characteristic to the right.

As the characteristic is traversed from high to low pressure ratio (i.e from the "stall side" to the "choke side" of the characteristic), the pressure untwist reduces. For the extent of the generated characteristics, the pressure untwist reduces by approximately 1.2° at the low and intermediate speeds for the analysed geometry. The partial characteristic at high speed displays a correspondingly small pressure untwist variation, namely 0.4°. Increasing the nozzle size at constant speed has a similar effect on the flow structure as increasing the speed at constant nozzle size; the shock moves rearward, toward the trailing edge of the blade, as can be seen in Fig. 7 and Fig. 8. As the shock moves rearward, the distribution of lift changes, thereby reducing the torque about an axis in the direction of the span of the blade. This results in the reduced pressure untwist displayed in Fig. 6.

The reduction in pressure untwist as the pressure ratio of the fan is lowered has an effect on the shape of the predicted characteristic. The CF+gas characteristic is steeper on the choke side than the CF-only case, where the blade geometry held fixed for all operating points. This is because the reduction in untwist results in a reduction in flow area, thereby lowering the mass-flow capacity of the fan. At high speed the characteristic has "fallen over", that is the mass-flow reduces with reducing pressure ratio. At the intermediate speed, a study was performed where the fan geometry was fixed at the CF+gas working line point and a characteristic generated. The fixed geometry blade passes 2.9% more flow than the dynamic untwist case. This highlights the importance of including the correct fan geometry when the pressure untwist is significant.

As can be immediately seen, including the tip-gap in the model only marginally influences the dynamic untwist behaviour of the nominal fan. The change in shape and location of the characteristics is comparable with the inviscid end-wall cases, as is the range of pressure untwist at each speed.

5 MIS-STAGGERED ASSEMBLY RESULTS

There are numerous geometric features of a fan blade that vary from one blade to another. The shape of the leading edge, thickness distribution, camber lines, stagger distribution and blade chord represent only a selection of parameters that can vary as a result of manufacturing limitations. Variation can also arise during assembly when blades are located at subtly different axial locations. Small variations in root location are magnified at the tip of the high aspect ratio blades. The tip stagger of a blade is intimately related to untwist, and is also a powerful aerodynamic parameter. For this reason, tip stagger was chosen as the variable feature between otherwise identical blades.

The stagger variation was achieved by modifying the stagger profile of individual blades in a linear fashion, applying zero displacement at the root and maximum stagger change at the tip. The deformations of blades rotating in a vacuum serve to reduce the stagger variation of an assembly relative to static conditions; a $\pm 0.35°$ static mis-stagger translates to a $\pm 0.26°$ mis-stagger at the intermediate shaft speed. However, the stagger variation changes by only 0.003° from the low the high speed

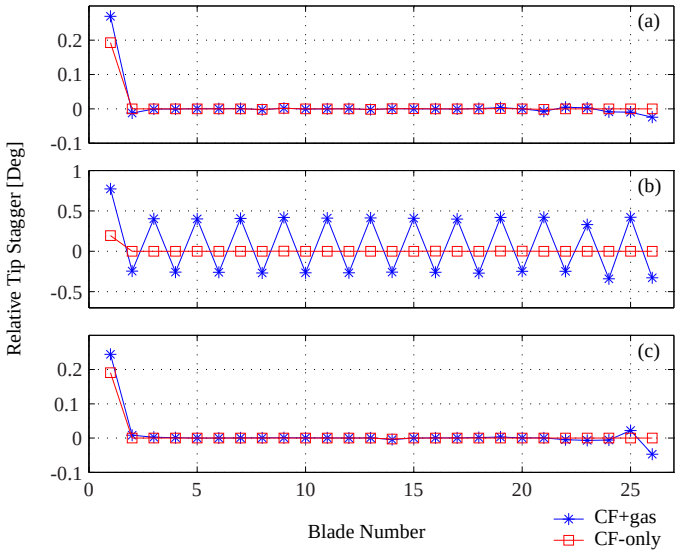

Figure 9. TIP STAGGER RELATIVE TO NOMINAL BLADE, BLADE 1 MIS-STAGGERED $(+0.2^\circ)$, (a) UNSTARTED, (b) INTERMEDIATE, (c) STARTED

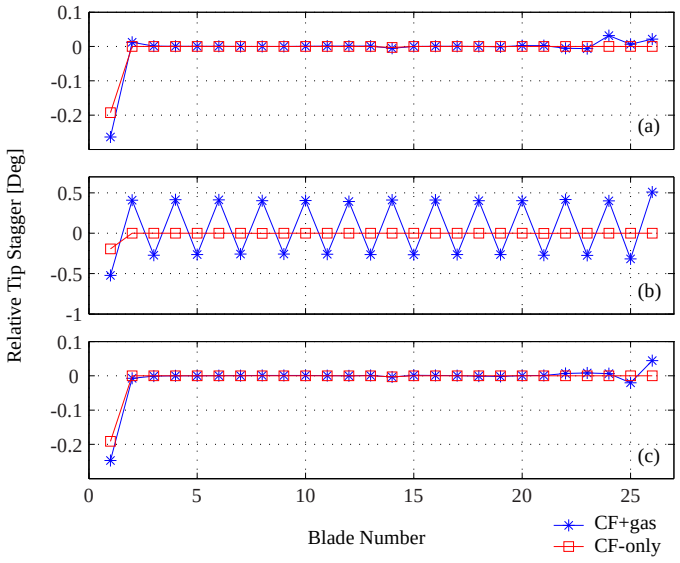

Figure 10. TIP STAGGER RELATIVE TO NOMINAL BLADE, BLADE 1 MIS-STAGGERED (-0.2°), (a) UNSTARTED, (b) INTERMEDIATE, (c) STARTED

cases studied here, for this level of static mis-stagger. As such all stagger variations were applied to the centrifugally displaced blades, acknowledging that this translates to a slightly larger static stagger variation. All mechanical properties of the blades were held fixed, ensuring that all observed effects originate from

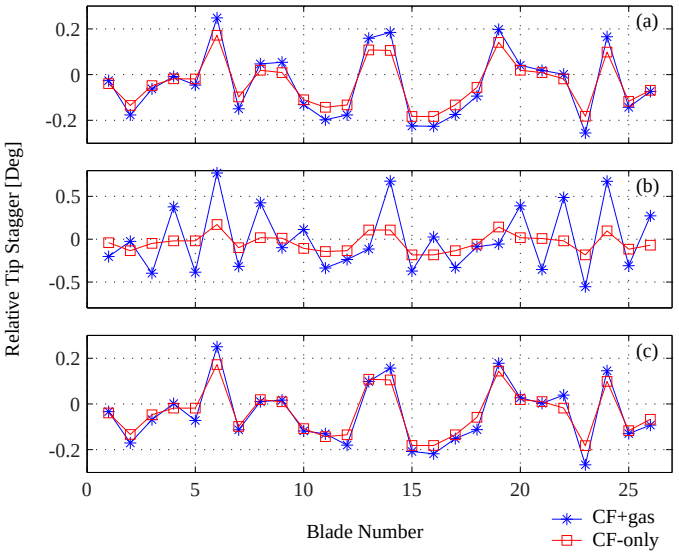

Figure 11. TIP STAGGER RELATIVE TO NOMINAL BLADE, RANDOM MIS-STAGGER, (a) UNSTARTED, (b) INTERMEDIATE, (c) STARTED

aerodynamic effects caused by the imposed geometric variability.

5.1 Unstarted and started flow

Untwist calculations for assemblies containing a solitary mis-staggered blade ($\pm 0.2^\circ$ tip stagger) were performed at both low and high shaft speeds corresponding to unstarted and started flow conditions respectively. The range of imposed mis-stagger is well within typical manufacturing tolerances. The results presented in this section are derived from calculations with inviscid end-walls, that is omitting the tip-gap. The CF-only and predicted CF+gas tip stagger patterns are shown in Fig. 9(a,c) and Fig. 10(a,c). The blades are numbered consecutively in the direction of rotation of the fan.

For both unstarted and started flow conditions, the presence of a solitary mis-staggered aerofoil in the assembly predominantly influences the untwist of the mis-staggered blade itself. The mis-stagger changes the passage geometries either side of the rogue blade, thereby changing the shock location on the pressure and suction surfaces of the blade . The mis-staggered blade is therefore subject to a lift distribution that is distinct from the nominal, and hence untwists differently. The aerofoils adjacent to the mis-staggered blade are also subjected to a different lift due to the passage geometry changes, and untwist accordingly. The first upstream blade, that is the blade adjacent to the mis-staggered blade in the direction of rotation, is only marginally influenced by the mis-staggered blade. The domain of influence extends further downstream to the second or third blade, depending on the operating condition. This suggests that geometry discrepancies in the passage adjacent to the suction

surface of the blade are most influential in terms of untwist. The change in untwist on all blades other than the mis-staggered blade is very subtle ($\pm 0.04^\circ$) and considerably lower than the imposed stagger variation of $\pm 0.2^\circ$. The resultant stagger patterns for the two cases studied display symmetry, that is the predicted pattern for the $+0.2^\circ$ case is approximately the same, up to a sign, as the predicted pattern for the -0.2° configuration.

Similar untwist calculations were performed for an assembly containing blades mis-staggered randomly in the range $[-0.2, 0.2]$. The CF-only and predicted CF+gas patterns are shown in Fig. 11(a,c). For both operating conditions the CF+gas pattern closely resembles the CF-only configuration. In general the most severely mis-staggered blades deviate from the CF-only pattern by the greatest margin. The CF-only stagger range increases by 42% and 45% after the aerodynamic loads have been accounted for, for unstarted and started flow respectively. The results show that the CF-only pattern can be used as a good approximation of the CF+gas configuration, provided that the nominal untwist is accounted for.

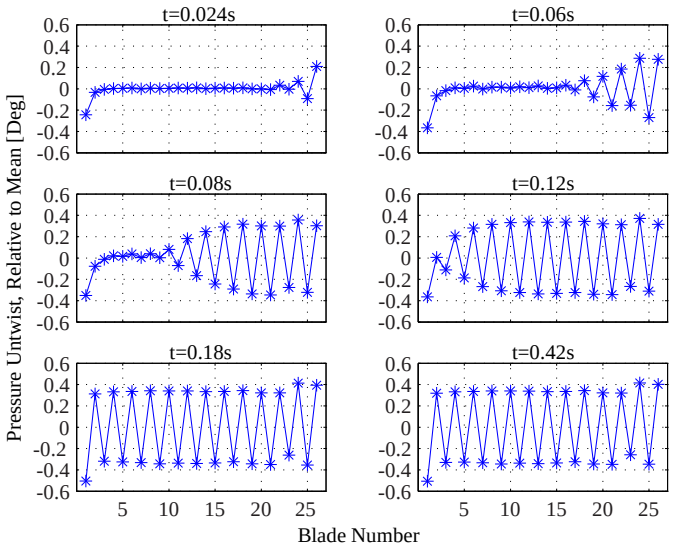

Figure 12. INTERMEDIATE SPEED PRESSURE UNTWIST SNAPSHOTS, BLADE 1 MIS-STAGGERED $(+0.2^\circ)$

5.2 Intermediate flow condition

Untwist calculations for the stagger patterns discussed in the previous subsection have been carried out at the intermediate shaft speed, near the transition between unstarted and started flow regimes. As above, the results here are derived from a model excluding the gap between the tip of the blade and the casing. At this operating point the shock wave forms near the leading edge of a nominal blade in a uniformly staggered assembly.

The CF-only and CF+gas stagger patterns for assemblies containing a solitary mis-staggered blade and a random assembly are shown in Figs. 9(b), 10(b), and 11(b). The contrast between the intermediate flow condition and the started and unstarted flow regimes discussed in the previous section is clear. Whereas for unstarted or started flow the domain of influence of a solitary mis-staggered blade is limited to its close neighbours, at the intermediate condition the untwist of every blade in the assembly is influenced by the mis-staggered blade. The CF+gas patterns shown in Fig. 9(b) and Fig. 10(b) overwhelm the prescribed CF-only mis-stagger, with a 0.2° mis-stagger resulting in a blade to blade pressure untwist variation of $\pm 0.54^\circ$, as opposed to $\pm 0.074^\circ$ for unstarted flow.

The generation of the "saw-tooth" pattern at the intermediate condition can be explained as follows. Consider the configuration comprising a single mis-staggered blade (denoted blade 1) that is closed by 0.2°, that is the stagger is increased by $+0.2^\circ$ relative to a nominal blade. As before the blades are numbered consecutively from 1 to 26 in the direction of rotation of the fan. The presence of the mis-staggered blade changes the geometry of both adjacent passages in the CF-only assembly. The shock wave in the passage adjacent to the pressure surface of the mis-staggered blade, that is the passage between blades 1 and 2, moves rearward toward the trailing edge as a result. Analogously, the shock wave in the passage between blades 26 and 1 moves forward, toward the leading edge. The change in lift distribution affects the untwist of the mis-staggered blade and also its immediate neighbours. The lift distribution of blade 2 is only marginally changed, due to a small movement of the shock on the suction surface, and so the untwist is only subtly affected. Blade 26, on the other hand, is subject to a larger change in lift relative to nominal, caused by the relatively large shock movement on the pressure surface, increasing the overall torque exerted by the gas about the span of the blade. The greater torque increases the pressure untwist of blade 26 relative to a nominal assembly. This in turn affects the geometry of the passage between blades 25 and 26, causing the shock to move rearward. The untwist of blade 25 is duly affected by the change in pressure surface shock position. At this operating condition the shock is very sensitive to mis-stagger. Indeed, it has been shown that the nominal equilibrium is unstable relative to mis-stagger [17]. The instability results in the unattenuated propagation of the pattern, in contrast to the localised disturbance from nominal for the started and unstarted flow conditions.

Figure 12 shows the unsteady process resulting in the saw-tooth pattern at the intermediate flow condition. After 0.024s the stagger pattern is reminiscent of the CF+gas pattern for started flow, although the variation from the mean is larger. The amplitude of the pressure untwist grows further, up to $\pm 0.35^\circ$, thereby extending the region of influence of the solitary mis-staggered blade. The saw-tooth pattern propagates around the entire annulus, in the direction opposite to the rotation of the

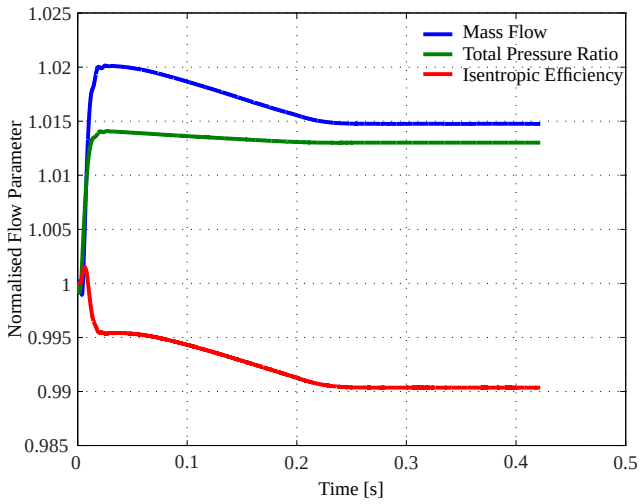

Figure 13. TIME EVOLUTION OF FLOW PARAMETERS, NORMALISED TO CF ONLY STEADY-STATE, INTERMEDIATE SPEED, BLADE 1 MIS-STAGGERED $(+0.2^\circ)$

fan, until the signal reaches the mis-staggered blade once more. The time-evolution of the mass-flow rate, total pressure ratio and isentropic efficiency of the fan during the unsteady process is shown in Fig. 13. Up to approximately 0.02s, the aerodynamic forces displace all blades away from the CF-only equilibrium. During this phase, the total pressure ratio and mass-flow rate increase while the isentropic efficiency decreases, in agreement with the results presented in section 4. Between approximately 0.02s and 0.25s the saw-tooth pattern propagates around the annulus, causing the mass-flow rate and isentropic efficiency of the fan to steadily reduce. The total pressure ratio of the fan also reduces slightly during this phase of the unsteady process.

A significant difference between the unstarted and started flow regimes and the intermediate flow condition is the correlation between the CF+gas and CF-only patterns for the random stagger pattern, shown in Fig. 11. As noted above, for unstarted and started flow the CF-only and CF+gas patterns are similar, differing only in variance. The correlation coefficient between the CF+gas and CF-only patterns for unstarted and started flows is high, at 0.99 and 0.98 respectively. At the intermediate flow condition, however, the CF-only and CF+gas stagger correlation drops substantially to 0.62, showing the significant change in the stagger pattern at this condition. This suggests that the CF-only stagger pattern cannot be directly used to infer a CF+gas stagger pattern at this operating condition.

The resultant saw-tooth pattern for an assembly containing a single mis-staggered blade strongly resembles the behaviour noted by Carstens and Belz [18], who observed a similar pattern emerging prior to a transonic cascade running into flutter. Carstens and Belz did not model any blade-to-blade variability, the pattern was produced as a result of the unsteady aerofoil vibration forcing the blades from the nominal unstable equilibrium.

5.3 Two mis-staggered blades

Figure 12 shows that when the saw-tooth pattern extends around the entire annulus and approaches the mis-staggered blade, it is in phase with itself. The even number of blades in the assembly ensure this is the case. This raises the question as to what would happen if the pattern was not in phase when it interacts with itself or another similar pattern. This is the case when two mis-staggered blades are introduced in an otherwise nominal assembly. One such configuration in the 26 blade assembly used in this study is where diametrically opposite blades are mis-staggered by $+0.2^\circ$. Let the mis-staggered blades be denoted by A and B. Allowing this configuration to untwist in response to the aerodynamic loads initially generates saw-tooth patterns emanating from both A and B. The pattern produced by A propagates until it reaches blade B. At this instant the pattern emanating from blade B is out of phase with that produced by A. As such, destructive interference occurs due to the changing pressure distribution on the pressure surface of blade B. This increases the pressure untwist of blade B toward the unstable nominal equilibrium, allowing the pattern generated by A to propagate past B. Due to the symmetry of the situation, the same process occurs at blade A in response to the pattern emanating from B. Therefore, when the pattern initially produced by blade A reaches blade A once more, it is out of phase. This once more initiates a destructive interference process, and the saw-tooth pattern propagation continues. The aeroelastic calculation proceeds until it eventually fails due to an accumulation of numerical errors generated by the mesh movement routine. As a result, no equilibrium between the fluid and the structure is found for this configuration.

The case with two mis-staggered blades that does not allow an equilibrium between the fluid and the structure may be idealised, but it introduces an interesting phenomenon. If, for example, the assembly analysed contained an odd number of blades, the cases containing a solitary mis-staggered blade would not have produced an equilibrium configuration. The randomly mis-staggered assembly analysed does have a running equilibrium. However, it is feasible, although not yet demonstrated, that an assembly where all blades are mis-staggered could be built that exhibits perpetual propagation of saw-tooth patterns at the intermediate shaft speed.

5.4 Mis-staggered fan performance

This section presents a comparison of the aerodynamic performance of mis-staggered and nominal fan assemblies. The total loss in the flow around transonic blades can be considered in two parts, the loss created by the shock and the blade profile loss [19]. The strong shock forming ahead of the blade passage

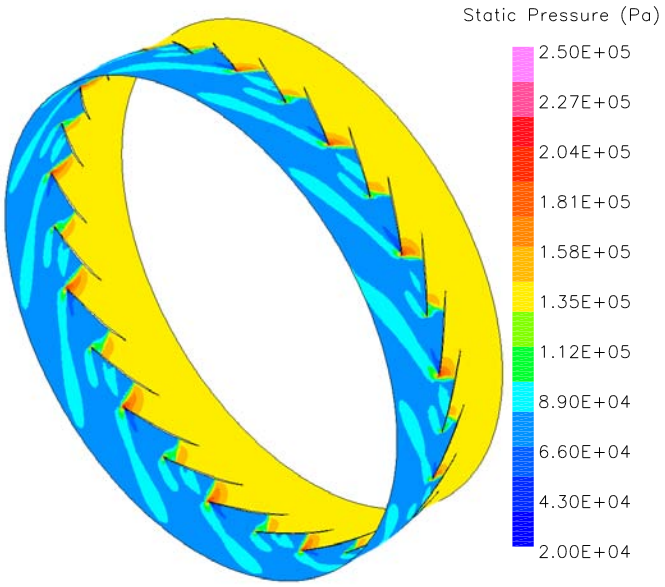

Figure 14. STATIC PRESSURE CONTOURS ON CASING FOR RUNNING GEOMETRY, NO TIP-GAP, ONE BLADE MIS-STAGGERED $(+0.2°)$.

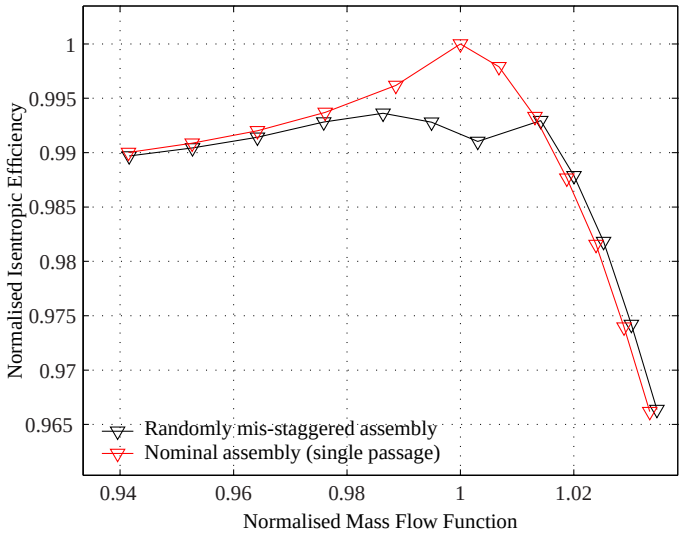

Figure 15. NOMINAL VS. RANDOMLY MIS-STAGGERED FAN ISENTROPIC EFFICIENCY ALONG WORKING LINE. MASS-FLOW AND EFFICIENCY NORMALISED RELATIVE TO INTERMEDIATE OPERATING POINT.

in unstarted flow dominates the total loss. For started flow the complex series of shock waves forming in the blade passage reduce the shock loss relative to the unstarted case, and the blade profile loss dominates. The intermediate speed, where the shock forms near the leading edge, balances the shock and profile losses and as such the fan is most efficient at this condition. This discussion is relevant to the case of a mis-staggered fan due to the untwist mechanism at the intermediate condition described above. The configurations containing a single mis-staggered blade form a saw-tooth pattern at the intermediate flow condition. The equilibrium flow comprises alternate started and unstarted passages, as shown in Fig. 14. Both started and unstarted passages generate a greater loss than nominal due to increased profile and shock losses respectively. The increased loss reduces the efficiency of the mis-staggered assembly by 0.7% of that of the nominal assembly.

Figure 15 shows the predicted isentropic efficiency of a nominal and a randomly mis-staggered assembly at a range of speeds between the unstarted and started flow conditions. The mass flow and efficiency are normalised relative to the intermediate flow condition. The same centrifugally displaced blade and the same mode-shapes are used at each of the speeds in this case. As such the change in blade shape due to the differing centrifugal loads is ignored, as are CF-stiffening effects. The results show that for unstarted and started flow conditions, occurring at low and high mass-flow respectively, the efficiency of the mis-staggered assembly matches that of the nominal. However, for a small speed range in the vicinity of the intermediate flow condition, the efficiency of the randomly mis-staggered assembly is reduced by a significant margin relative to the nominal assembly. The loss in efficiency of 0.72% of nominal is comparable with that observed for the configuration containing a solitary mis-staggered blade.

5.5 Tip-gap effects

Including a representation of the tip-gap in the untwist prediction model was shown in section 4 not to alter the untwist behaviour of a nominal fan. However, it remains to be shown that the tip-gap effects in a mis-staggered fan assembly are significant or otherwise.

The position of the shock near the tip of the blade is influenced by the over-tip flow. It does not immediately follow, therefore, that the shock position at the intermediate flow condition will display the same properties as the inviscid end-wall case. To investigate the effect of including the tip-gap in the model, a tip-gap was added to the randomly mis-staggered assembly used in the previous section. The same gap between each centrifugally displaced blade and the casing was imposed, that is each blade has the same tip-gap before it is allowed to deform in response to the pressure loads. In reality, the gap between each blade and the casing will vary, but the investigation into this form of variability is beyond the scope of this paper. However, as each blade in a mis-staggered assembly untwists

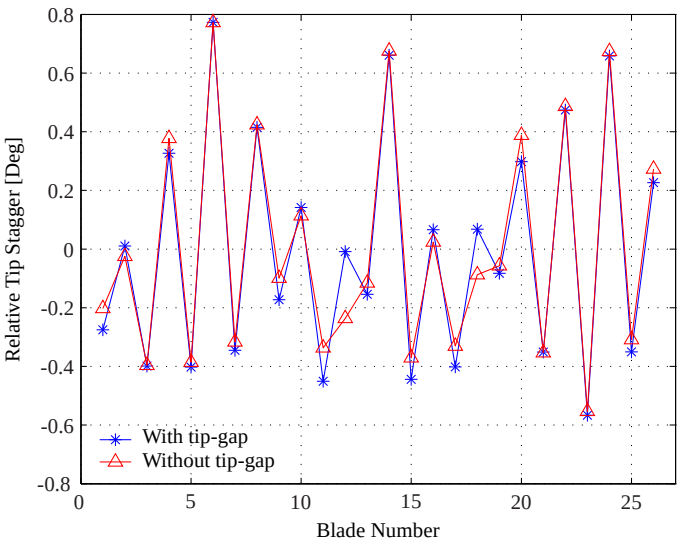

Figure 16. TIP STAGGER RELATIVE TO NOMINAL BLADE, RANDOM MIS-STAGGER, WITH AND WITHOUT TIP-GAP

differently, the tip-gap at the final equilibrium position will vary from blade to blade.

The final equilibrium stagger of the mis-staggered assembly is shown for both cases with and without a tip-gap in Fig. 16. The two resultant patterns are very similar, differing only in subtle detail. As it is difficult to obtain precisely equivalent operating conditions for the two cases, it is not surprising that they differ slightly. The result shows that the sensitivity of the shock position with respect to small levels of mis-stagger is not reduced by the influence of the tip-gap. This does not mean that the shock position is unaffected by the tip-gap, rather the change in blade loading with respect to mis-stagger is insensitive to the presence of the tip-gap. It is therefore concluded that a model excluding the tip-gap, which is computationally more efficient, is adequate for the purpose of untwist prediction. In the authors' opinion, this is a general result and not specific to the this case.

6 CONCLUSIONS

An integrated, non-linear aeroelastic code has been used to predict the effect of stagger variability in gas turbine fan assemblies at sea-level. An analysis of a nominal assembly has also been given. The main conclusions of the study are as follows:

1. As both a constant speed characteristic and a working line is traversed at sea level, the change in blade shape due to the varying aerodynamic loads is significant. The common practise of using a constant blade shape to analyse a characteristic is shown to produce significantly different results relative to the dynamic untwist calculations.
2. The equilibrium stagger pattern at both unstarted and started flow conditions closely resembles the prescribed CF-only pattern. The pressure untwist of the most heavily mis-staggered blades deviate from nominal by the greatest margin.
3. At the intermediate flow condition the presence of a single mis-staggered blade can influence the pressure untwist of every blade in the assembly. For certain configurations this can produce an unstable condition with no equilibrium between the structure and the fluid. The CF+gas equilibrium stagger pattern for a randomly mis-staggered assembly correlates poorly with the CF-only pattern, in contrast to the unstarted and started flow conditions.
4. The isentropic efficiency of a mis-staggered fan is substantially reduced in the vicinity of the intermediate operating condition, relative to a nominal assembly.
5. The inclusion of a tip-gap in the aeroelastic model does not significantly change the predicted untwist behaviour.

ACKNOWLEDGMENT

The authors would like to thank Rolls-Royce plc for both sponsoring this work and allowing its publication. The support of the DTI (project number TP/2/ET/6/I/10073) is also gratefully acknowledged.

REFERENCES

[1] Fleeter, S., and Hoyniak, D., 1986. "Forced response analysis of an aerodynamically detuned supersonic turbomachine rotor". *ASME Journal of Vibration Acoustics Stress and Reliability in Design*, **108**(2), pp. 117–124.

[2] Fleeter, S., and Hoyniak, D., 1986. "Aerodynamic detuning analysis of an unstalled supersonic turbofan cascade". *ASME Journal of Engineering for Gas Turbines and Power*, **108**(1), pp. 60–67.

[3] Stratford, B. S., and Newby, D. R., 1977. "A new look at the generation of buzz-saw noise". *AIAA Paper*, **AIAA-1977-1343**.

[4] Roberts, W. B., Armin, A., Kassaseya, G., Suder, K. L., Thorp, S. A., and Strazisar, A. J., 2002. "The effect of variable chord length on transonic axial rotor performance". *ASME Journal of Turbomachinery*, **124**(3), pp. 351–357.

[5] Roehle, I., Le Guevel, A., and Fradin, C., 1999. "3D-shock visualisation in a transonic compressor rotor". *Optics and Laser Tchnology*, **31**(1), pp. 67–73.

[6] Kamakoti, R., and Shyy, W., 2004. "Fluid-structure interaction for aeroelastic applications". *Progress in Aerospace Sciences*, **40**, pp. 535–558.

[7] Yamamoto, O., and August, R., 1992. "Structural and

aerodynamic analysis of a large-scale advanced propeller blade". *Journal of Propulsion and Power,* **8**(2), pp. 367–373.

[8] Srivastava, R., Sankar, L. N., Reddy, T. S. R., and Huff, D. L., 1991. "Application of an efficient hybrid scheme for aeroelastic analysis of advanced propellers". *Journal of Propulsion and Power,* **7**(5), pp. 767–775.

[9] Guruswamy, G. P., 1989. "Integrated approach for active coupling of fluids and structures". *AIAA Journal,* **27**(6), pp. 788–793.

[10] Marshall, J. G., 1996. "Prediction of turbomachinery aeroelasticity effects using a 3D nonlinear integrated method". PhD thesis, Imperial College of Science, Technology and Medicine, University of London.

[11] Sayma, A. I., Vahdati, M., and Imregun, M., 2000. "An integrated non-linear approach for turbomachinery forced response prediction - part 1: formulation". *Journal of Fluids and Structures,* **14**(1), pp. 87–101.

[12] Sayma, A. I., Vahdati, M., Sbardella, L., and Imregun, M., 2000. "Modelling of 3D viscous compressible turbomachinery flows using unstructured hybrid grids". *AIAA Journal,* **38**(6), pp. 945–954.

[13] Sbardella, L., Sayma, A. I., and Imregun, M., 2000. "Semi-unstructured meshes for axial turbomachine blades". *International Journal of Numerical Methods in Fluids,* **32**(5), pp. 569–584.

[14] Spalart, P. R., and Allmaras, S. R., 1992. "A one-equation turbulence model for aerodynamic flows". *AIAA Paper,* **AIAA-1992-0439**.

[15] Batina, J. T., 1991. "Unsteady Euler algorithm with unstructured dynamic mesh for complex-aircraft aerodynamic analysis". *AIAA Journal,* **29**(3), pp. 327–333.

[16] Robinson, B. A., Batina, J. T., and Yang, H. T. Y., 1991. "Aeroelastic analysis of wings using the Euler equations with a deforming mesh". *Journal of Aircraft,* **28**(11), pp. 781–788.

[17] Wilson, M. J., Imregun, M., and Sayma, A. I., 2005. "The effect of stagger variability in gas turbine fan assemblies". In International conference on compressors and their systems, 4-7 september 2005, Institution of Mechanical Engineers, pp. 507–515.

[18] Carstens, V., and Belz, J., 2001. "Numerical investigation of nonlinear fluid-structure interaction in vibrating compressor blades". *ASME Journal of Turbomachinery,* **123**(2), pp. 402–408.

[19] Cumpsty, N. A., 1989. *Compressor aerodynamics*. Longman Scientific & Technical, UK.